[Van87], [Zog87], [Sei91]) and is useful for predicting receiver power which scatters off large objects, such as buildings, which are for both the transmitter and receiver.

Several European cities were measured from the perimeter [Sei91], and *RCS* values for several buildings were determined from measured power delay profiles. For medium and large size buildings located 5 - 10 km away, *RCS* values were found to be in the range of $14.1 dB \cdot m^2$ to $55.7\ dB \cdot m^2$.

3.9 Practical Link Budget Design using Path Loss Models

Most radio propagation models are derived using a combination of analytical and empirical methods. The empirical approach is based on fitting curves or analytical expressions that recreate a set of measured data. This has the advantage of implicitly taking into account all propagation factors, both known and unknown, through actual field measurements. However, the validity of an empirical model at transmission frequencies or environments other than those used to derive the model can only be established by additional measured data in the new environment at the required transmission frequency. Over time, some classical propagation models have emerged, which are now used to predict large-scale coverage for mobile communication systems design. By using path loss models to estimate the received signal level as a function of distance, it becomes possible to predict the SNR for a mobile communication system. Using noise analysis techniques given in Appendix B, the noise floor can be determined. For example, the 2-ray model described in section 3.6 was used to estimate capacity in a spread spectrum cellular system, before such systems were deployed [Rap92b]. Practical path loss estimation techniques are now presented.

3.9.1 Log-distance Path Loss Model

Both theoretical and measurement-based propagation models indicate that average received signal power decreases logarithmically with distance, whether in outdoor or indoor radio channels. Such models have been used extensively in the literature. The average large-scale path loss for an arbitrary T-R separation is expressed as a function of distance by using a path loss exponent, n.

$$\overline{PL}(d) \propto \left(\frac{d}{d_0}\right)^n \tag{3.67}$$

or

$$\overline{PL}(\text{dB}) = \overline{PL}(d_0) + 10n\log\left(\frac{d}{d_0}\right) \tag{3.68}$$

where n is the path loss exponent which indicates the rate at which the path loss increases with distance, d_0 is the close-in reference distance which is determined from measurements close to the transmitter, and d is the T-R separation

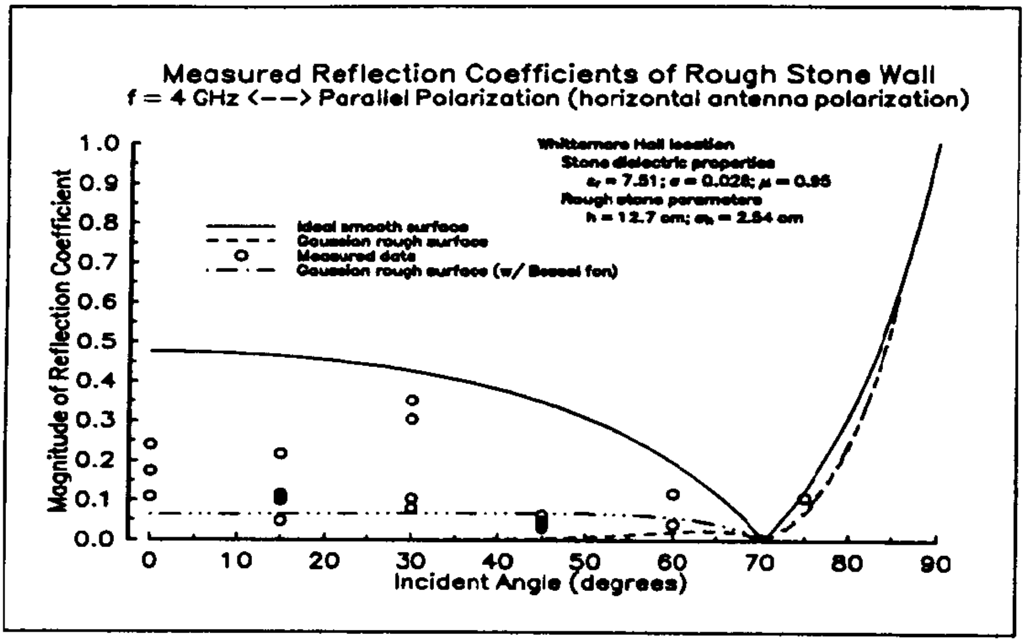

(a) E-field in the plane of incidence. (parallel polarization)

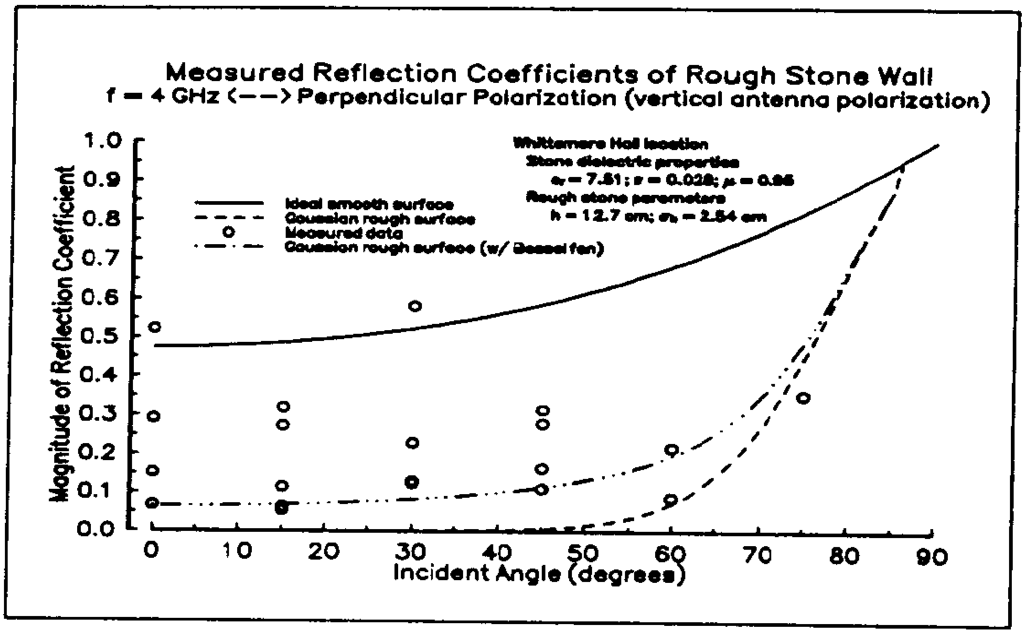

(b) E-field normal to plane of incidence. (perpendicular polarization)

Figure 3.16
Measured reflection coefficients versus incident angle at a rough stone wall site. In these graphs, incident angle is measured with respect to the normal, instead of with respect to the surface boundary as defined in Figure 3.4. These graphs agree with Figure 3.6 [Lan96].

distance. The bars in equations (3.67) and (3.68) denote the ensemble average of all possible path loss values for a given value of d. When plotted on a log-log scale, the modeled path loss is a straight line with a slope equal to $10n$ dB per decade. The value of n depends on the specific propagation environment. For example, in free space, n is equal to 2, and when obstructions are present, n will have a larger value.

It is important to select a free space reference distance that is appropriate for the propagation environment. In large coverage cellular systems, 1 km reference distances are commonly used [Lee85], whereas in microcellular systems, much smaller distances (such as 100 m or 1 m) are used. The reference distance should always be in the far field of the antenna so that near-field effects do not alter the reference path loss. The reference path loss is calculated using the free space path loss formula given by equation (3.5) or through field measurements at distance d_0. Table 3.2 lists typical path loss exponents obtained in various mobile radio environments.

Table 3.2 Path Loss Exponents for Different Environments

Environment	Path Loss Exponent, n
Free space	2
Urban area cellular radio	2.7 to 3.5
Shadowed urban cellular radio	3 to 5
In building line-of-sight	1.6 to 1.8
Obstructed in building	4 to 6
Obstructed in factories	2 to 3

3.9.2 Log-normal Shadowing

The model in equation (3.68) does not consider the fact that the surrounding environmental clutter may be vastly different at two different locations having the same T-R separation. This leads to measured signals which are vastly different than the *average* value predicted by equation (3.68). Measurements have shown that at any value of d, the path loss $PL(d)$ at a particular location is random and distributed log-normally (normal in dB) about the mean distance-dependent value [Cox84], [Ber87]. That is

$$PL(d)[dB] = \overline{PL}(d) + X_\sigma = \overline{PL}(d_0) + 10n\log\left(\frac{d}{d_0}\right) + X_\sigma \qquad (3.69.a)$$

and

$$P_r(d)[dBm] = P_t[dBm] - PL(d)[dB] \text{ (antenna gains included in } PL(d)) \qquad (3.69.b)$$

where X_σ is a zero-mean Gaussian distributed random variable (in dB) with standard deviation σ (also in dB).

The log-normal distribution describes the random *shadowing* effects which occur over a large number of measurement locations which have the same T-R separation, but have different levels of clutter on the propagation path. This phenomenon is referred to as *log-normal shadowing*. Simply put, log-normal shadowing implies that measured signal levels at a specific T-R separation have a Gaussian (normal) distribution about the distance-dependent mean of (3.68), where the measured signal levels have values in dB units. The standard deviation of the Gaussian distribution that describes the shadowing also has units in dB. Thus, the random effects of shadowing are accounted for using the Gaussian distribution which lends itself readily to evaluation (see Appendix D).

The close-in reference distance d_0, the path loss exponent n, and the standard deviation σ, statistically describe the path loss model for an arbitrary location having a specific T-R separation, and this model may be used in computer simulation to provide received power levels for random locations in communication system design and analysis.

In practice, the values of n and σ are computed from measured data, using linear regression such that the difference between the measured and estimated path losses is minimized in a mean square error sense over a wide range of measurement locations and T-R separations. The value of $\overline{PL}(d_0)$ in (3.69.a) is based on either close-in measurements or on a free space assumption from the transmitter to d_0. An example of how the path loss exponent is determined from measured data follows. Figure 3.17 illustrates actual measured data in several cellular radio systems and demonstrates the random variations about the mean path loss (in dB) due to shadowing at specific T-R separations.

Since $PL(d)$ is a random variable with a normal distribution in dB about the distance-dependent mean, so is $P_r(d)$, and the Q-function or error function (*erf*) may be used to determine the probability that the received signal level will exceed (or fall below) a particular level. The Q-function is defined as

$$Q(z) = \frac{1}{\sqrt{2\pi}}\int_z^{\infty} \exp\left(-\frac{x^2}{2}\right)dx = \frac{1}{2}\left[1 - erf\left(\frac{z}{\sqrt{2}}\right)\right] \tag{3.70.a}$$

where

$$Q(z) = 1 - Q(-z) \tag{3.70.b}$$

The probability that the received signal level will exceed a certain value γ can be calculated from the cumulative density function as

$$Pr[P_r(d) > \gamma] = Q\left(\frac{\gamma - \overline{P_r(d)}}{\sigma}\right) \tag{3.71}$$

Similarly, the probability that the received signal level will be below γ is given by

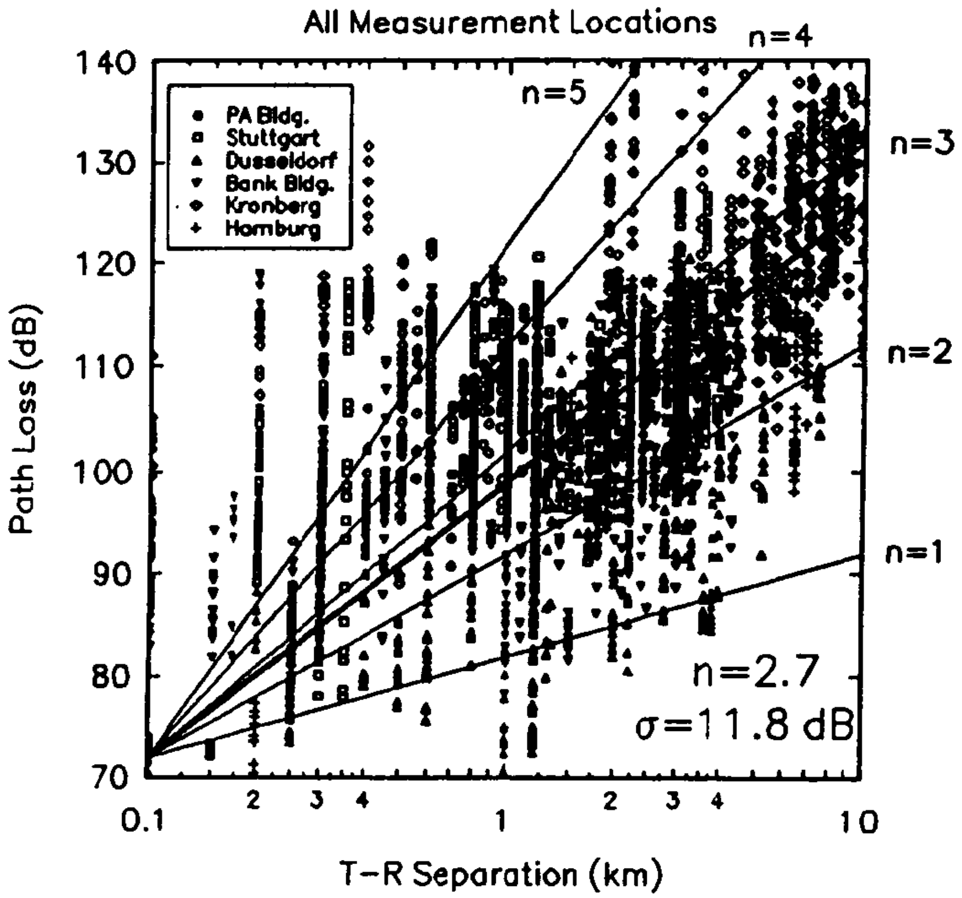

Figure 3.17
Scatter plot of measured data and corresponding MMSE path loss model for many cities in Germany. For this data, $n = 2.7$ and $\sigma = 11.8$ dB [From [Sei91] © IEEE].

$$Pr[P_r(d) < \gamma] = Q\left(\frac{\overline{P_r(d)} - \gamma}{\sigma}\right) \tag{3.72}$$

Appendix D provides tables for evaluating the Q and erf functions.

3.9.3 Determination of Percentage of Coverage Area

It is clear that due to random effects of shadowing, some locations within a coverage area will be below a particular desired received signal threshold. It is often useful to compute how the boundary coverage relates to the percent of area covered within the boundary. For a circular coverage area having radius R from a base station, let there be some desired received signal threshold γ. We are interested in computing $U(\gamma)$, the percentage of useful service area (i.e. the percentage of area with a received signal that is equal or greater than γ), given a

CHAPTER 4

Mobile Radio Propagation: Small-Scale Fading and Multipath

Small-scale fading, or simply *fading*, is used to describe the rapid fluctuation of the amplitude of a radio signal over a short period of time or travel distance, so that large-scale path loss effects may be ignored. Fading is caused by interference between two or more versions of the transmitted signal which arrive at the receiver at slightly different times. These waves, called *multipath waves*, combine at the receiver antenna to give a resultant signal which can vary widely in amplitude and phase, depending on the distribution of the intensity and relative propagation time of the waves and the bandwidth of the transmitted signal.

4.1 Small-Scale Multipath Propagation

Multipath in the radio channel creates small-scale fading effects. The three most important effects are:

- Rapid changes in signal strength over a small travel distance or time interval
- Random frequency modulation due to varying Doppler shifts on different multipath signals
- Time dispersion (echoes) caused by multipath propagation delays.

In built-up urban areas, fading occurs because the height of the mobile antennas are well below the height of surrounding structures, so there is no single line-of-sight path to the base station. Even when a line-of-sight exists, multipath still occurs due to reflections from the ground and surrounding structures. The incoming radio waves arrive from different directions with different propagation delays. The signal received by the mobile at any point in space may consist of a large number of plane waves having randomly distributed amplitudes, phases, and angles of arrival. These multipath components combine vectorially at the receiver antenna, and can cause the signal received by the mobile to distort or fade. Even when a mobile receiver is stationary, the received signal may fade due to movement of surrounding objects in the radio channel.

If objects in the radio channel are static, and motion is considered to be only due to that of the mobile, then fading is purely a spatial phenomenon. The spatial variations of the resulting signal are seen as temporal variations by the receiver as it moves through the multipath field. Due to the constructive and destructive effects of multipath waves summing at various points in space, a receiver moving at high speed can pass through several fades in a small period of time. In a more serious case, a receiver may stop at a particular location at which the received signal is in a deep fade. Maintaining good communications can then become very difficult, although passing vehicles or people walking in the vicinity of the mobile can often disturb the field pattern, thereby diminishing the likelihood of the received signal remaining in a deep null for a long period of time. Antenna space diversity can prevent deep fading nulls, as shown in Chapter 6. Figure 3.1 shows typical rapid variations in the received signal level due to small-scale fading as a receiver is moved over a distance of a few meters.

Due to the relative motion between the mobile and the base station, each multipath wave experiences an apparent shift in frequency. The shift in received signal frequency due to motion is called the Doppler shift, and is directly proportional to the velocity and direction of motion of the mobile with respect to the direction of arrival of the received multipath wave.

4.1.1 Factors Influencing Small-Scale Fading

Many physical factors in the radio propagation channel influence small-scale fading. These include the following:

- **Multipath propagation** — The presence of reflecting objects and scatterers in the channel creates a constantly changing environment that dissipates the signal energy in amplitude, phase, and time. These effects result in multiple versions of the transmitted signal that arrive at the receiving antenna, displaced with respect to one another in time and spatial orientation. The random phase and amplitudes of the different multipath components cause fluctuations in signal strength, thereby inducing small-scale fading, signal distortion, or both. Multipath propagation often lengthens the time required for the baseband portion of the signal to reach the receiver which can cause signal smearing due to intersymbol interference.
- **Speed of the mobile** — The relative motion between the base station and the mobile results in random frequency modulation due to different Doppler shifts on each of the multipath components. Doppler shift will be positive or negative depending on whether the mobile receiver is moving toward or away from the base station.

- **Speed of surrounding objects** — If objects in the radio channel are in motion, they induce a time varying Doppler shift on multipath components. If the surrounding objects move at a greater rate than the mobile, then this effect dominates the small-scale fading. Otherwise, motion of surrounding objects may be ignored, and only the speed of the mobile need be considered.
- **The transmission bandwidth of the signal** — If the transmitted radio signal bandwidth is greater than the "bandwidth" of the multipath channel, the received signal will be distorted, but the received signal strength will not fade much over a local area (i.e., the small-scale signal fading will not be significant). As will be shown, the bandwidth of the channel can be quantified by the *coherence bandwidth* which is related to the specific multipath structure of the channel. The coherence bandwidth is a measure of the maximum frequency difference for which signals are still strongly correlated in amplitude. If the transmitted signal has a narrow bandwidth as compared to the channel, the amplitude of the signal will change rapidly, but the signal will not be distorted in time. Thus, the statistics of small-scale signal strength and the likelihood of signal smearing appearing over small-scale distances are very much related to the specific amplitudes and delays of the multipath channel, as well as the bandwidth of the transmitted signal.

4.1.2 Doppler Shift

Consider a mobile moving at a constant velocity v, along a path segment having length d between points X and Y, while it receives signals from a remote source S, as illustrated in Figure 4.1. The difference in path lengths traveled by the wave from source S to the mobile at points X and Y is $\Delta l = d\cos\theta = v\Delta t\cos\theta$, where Δt is the time required for the mobile to travel from X to Y, and θ is assumed to be the same at points X and Y since the source is assumed to be very far away. The phase change in the received signal due to the difference in path lengths is therefore

$$\Delta\phi = \frac{2\pi\Delta l}{\lambda} = \frac{2\pi v\Delta t}{\lambda}\cos\theta \qquad (4.1)$$

and hence the apparent change in frequency, or Doppler shift, is given by f_d, where

$$f_d = \frac{1}{2\pi}\cdot\frac{\Delta\phi}{\Delta t} = \frac{v}{\lambda}\cdot\cos\theta \qquad (4.2)$$

Equation (4.2) relates the Doppler shift to the mobile velocity and the spatial angle between the direction of motion of the mobile and the direction of arrival of the wave. It can be seen from equation (4.2) that if the mobile is moving toward the direction of arrival of the wave, the Doppler shift is positive (i.e., the apparent received frequency is increased), and if the mobile is moving away from the direction of arrival of the wave, the Doppler shift is negative (i.e. the apparent received frequency is decreased). As shown in section 4.7.1, multipath components from a CW signal which arrive from different directions contribute to Doppler spreading of the received signal, thus increasing the signal bandwidth.

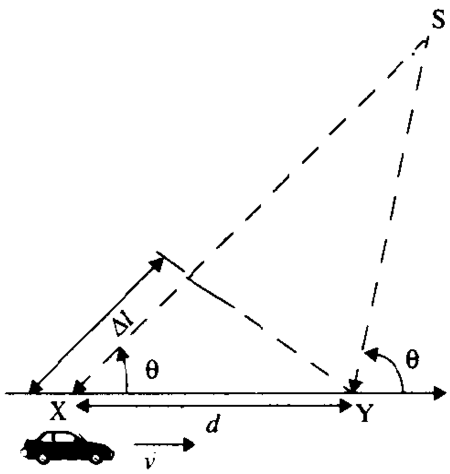

Figure 4.1
Illustration of Doppler effect.

Example 4.1

Consider a transmitter which radiates a sinusoidal carrier frequency of 1850 MHz. For a vehicle moving 60 mph, compute the received carrier frequency if the mobile is moving (a) directly towards the transmitter, (b) directly away from the transmitter, (c) in a direction which is perpendicular to the direction of arrival of the transmitted signal.

Solution to Example 4.1

Given:

Carrier frequency $f_c = 1850\,\text{MHz}$

Therefore, wavelength $\lambda = c/f_c = \dfrac{3 \times 10^8}{1850 \times 10^6} = 0.162\,\text{m}$

Vehicle speed $v = 60$ mph $= 26.82$ m/s

(a) The vehicle is moving directly towards the transmitter.
The Doppler shift in this case is positive and the received frequency is given by equation (4.2)

$$f = f_c + f_d = 1850 \times 10^6 + \frac{26.82}{0.162} = 1850.00016\ \text{MHz}$$

(b) The vehicle is moving directly away from the transmitter.
The Doppler shift in this case is negative and hence the received frequency is given by

$$f = f_c - f_d = 1850 \times 10^6 - \frac{26.82}{0.162} = 1849.999834 \text{ MHz}$$

(c) The vehicle is moving perpendicular to the angle of arrival of the transmitted signal.
In this case, $\theta = 90°$, $\cos\theta = 0$, and there is no Doppler shift.
The received signal frequency is the same as the transmitted frequency of 1850 MHz.

4.2 Impulse Response Model of a Multipath Channel

The small-scale variations of a mobile radio signal can be directly related to the impulse response of the mobile radio channel. The impulse response is a wideband channel characterization and contains all information necessary to simulate or analyze any type of radio transmission through the channel. This stems from the fact that a mobile radio channel may be modeled as a linear filter with a time varying impulse response, where the time variation is due to receiver motion in space. The filtering nature of the channel is caused by the summation of amplitudes and delays of the multiple arriving waves at any instant of time. The impulse response is a useful characterization of the channel, since it may be used to predict and compare the performance of many different mobile communication systems and transmission bandwidths for a particular mobile channel condition.

To show that a mobile radio channel may be modeled as a linear filter with a time varying impulse response, consider the case where time variation is due strictly to receiver motion in space. This is shown in Figure 4.2.

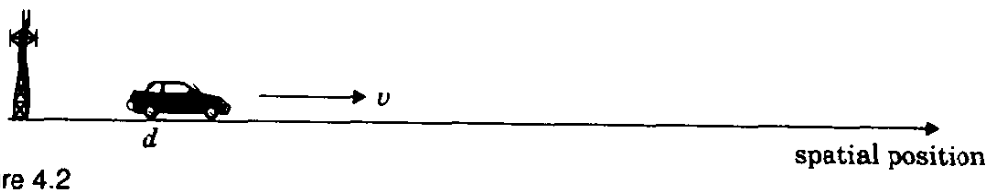

Figure 4.2
The mobile radio channel as a function of time and space.

In Figure 4.2, the receiver moves along the ground at some constant velocity v. For a fixed position d, the channel between the transmitter and the receiver can be modeled as a linear time invariant system. However, due to the different multipath waves which have propagation delays which vary over different spatial locations of the receiver, the impulse response of the linear time invariant channel should be a function of the position of the receiver. That is, the channel impulse response can be expressed as $h(d,t)$. Let $x(t)$ represent the transmitted signal, then the received signal $y(d,t)$ at position d can be expressed as a convolution of $x(t)$ with $h(d,t)$.

$$y(d,t) = x(t) \otimes h(d,t) = \int_{-\infty}^{\infty} x(\tau)h(d,t-\tau)d\tau \tag{4.3}$$

For a causal system, $h(d,t) = 0$ for $t<0$, thus equation (4.3) reduces to

$$y(d,t) = \int_{-\infty}^{t} x(\tau)h(d,t-\tau)d\tau \tag{4.4}$$

Since the receiver moves along the ground at a constant velocity v, the position of the receiver can by expressed as

$$d = vt \tag{4.5}$$

Substituting (4.5) in (4.4), we obtain

$$y(vt,t) = \int_{-\infty}^{t} x(\tau)h(vt,t-\tau)d\tau \tag{4.6}$$

Since v is a constant, $y(vt,t)$ is just a function of t. Therefore, equation (4.6) can be expressed as

$$y(t) = \int_{-\infty}^{t} x(\tau)h(vt,t-\tau)d\tau = x(t) \otimes h(vt,t) = x(t) \otimes h(d,t) \tag{4.7}$$

From equation (4.7) it is clear that the mobile radio channel can be modeled as a linear time varying channel, where the channel changes with time and distance.

Since v may be assumed constant over a short time (or distance) interval, we may let $x(t)$ represent the transmitted bandpass waveform, $y(t)$ the received waveform, and $h(t,\tau)$ the impulse response of the time varying multipath radio channel. The impulse response $h(t,\tau)$ completely characterizes the channel and is a function of both t and τ. The variable t represents the time variations due to motion, whereas τ represents the channel multipath delay for a fixed value of t. One may think of τ as being a vernier adjustment of time. The received signal $y(t)$ can be expressed as a convolution of the transmitted signal $x(t)$ with the channel impulse response (see Figure 4.3a).

$$y(t) = \int_{-\infty}^{\infty} x(\tau)h(t,\tau)d\tau = x(t) \otimes h(t,\tau) \tag{4.8}$$

If the multipath channel is assumed to be a bandlimited bandpass channel, which is reasonable, then $h(t,\tau)$ may be equivalently described by a complex baseband impulse response $h_b(t,\tau)$ with the input and output being the complex envelope representations of the transmitted and received signals, respectively (see Figure 4.3b). That is,

$$r(t) = c(t) \otimes \frac{1}{2}h_b(t,\tau) \tag{4.9}$$

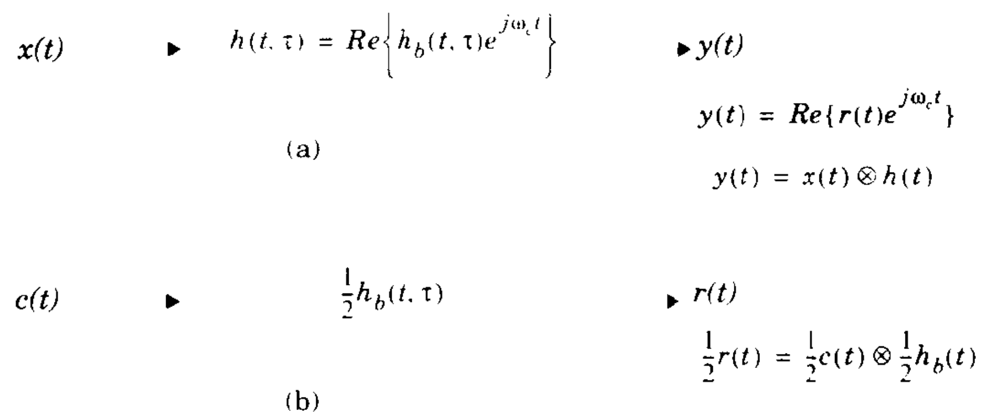

Figure 4.3
(a) Bandpass channel impulse response model.
(b) Baseband equivalent channel impulse response model.

where $c(t)$ and $r(t)$ are the complex envelopes of $x(t)$ and $y(t)$, defined as

$$x(t) = Re\{c(t)\exp(j2\pi f_c t)\} \quad (4.10)$$

$$y(t) = Re\{r(t)\exp(j2\pi f_c t)\} \quad (4.11)$$

The factor of $1/2$ in equation (4.9) is due to the properties of the complex envelope, in order to represent the passband radio system at baseband. The low-pass characterization removes the high frequency variations caused by the carrier, making the signal analytically easier to handle. It is shown by Couch [Cou93] that the average power of a bandpass signal $\overline{x^2(t)}$ is equal to $\frac{1}{2}\overline{|c(t)|^2}$, where the overbar denotes ensemble average for a stochastic signal, or time average for a deterministic or ergodic stochastic signal.

It is useful to discretize the multipath delay axis τ of the impulse response into equal time delay segments called *excess delay bins*, where each bin has a time delay width equal to $\tau_{i+1} - \tau_i$, where τ_0 is equal to 0, and represents the first arriving signal at the receiver. Letting i = 0, it is seen that $\tau_1 - \tau_0$ is equal to the time delay bin width given by $\Delta\tau$. For convention, $\tau_0 = 0$, $\tau_1 = \Delta\tau$, and $\tau_i = i\Delta\tau$, for $i = 0$ to $N-1$, where N represents the total number of possible equally-spaced multipath components, including the first arriving component. Any number of multipath signals received within the i th bin are represented by a single resolvable multipath component having delay τ_i. This technique of quantizing the delay bins determines the time delay resolution of the channel model, and the useful frequency span of the model can be shown to be $1/(2\Delta\tau)$. That is, the model may be used to analyze transmitted signals having bandwidths which are less than $1/(2\Delta\tau)$. Note that $\tau_0 = 0$ is the excess time delay of the first arriving multipath component, and neglects the propagation delay between the transmitter and receiver. *Excess delay* is the relative delay of the i th multipath component as compared to the first arriving component and is given by τ_i. The *maximum excess delay* of the channel is given by $N\Delta\tau$.

Since the received signal in a multipath channel consists of a series of attenuated, time-delayed, phase shifted replicas of the transmitted signal, the baseband impulse response of a multipath channel can be expressed as

$$h_b(t, \tau) = \sum_{i=0}^{N-1} a_i(t, \tau)\exp[j(2\pi f_c\tau_i(t) + \phi_i(t, \tau))]\delta(\tau - \tau_i(t)) \tag{4.12}$$

where $a_i(t, \tau)$ and $\tau_i(t)$ are the real amplitudes and excess delays, respectively, of i th multipath component at time t [Tur72]. The phase term $2\pi f_c\tau_i(t) + \phi_i(t, \tau)$ in (4.12) represents the phase shift due to free space propagation of the i th multipath component, plus any additional phase shifts which are encountered in the channel. In general, the phase term is simply represented by a single variable $\theta_i(t, \tau)$ which lumps together all the mechanisms for phase shifts of a single multipath component within the ith excess delay bin. Note that some excess delay bins may have no multipath at some time t and delay τ_i, since $a_i(t, \tau)$ may be zero. In equation (4.12), N is the total possible number of multipath components (bins), and $\delta(\bullet)$ is the unit impulse function which determines the specific multipath bins that have components at time t and excess delays τ_i. Figure 4.4 illustrates an example of different snapshots of $h_b(t, \tau)$, where t varies into the page, and the time delay bins are quantized to widths of $\Delta\tau$.

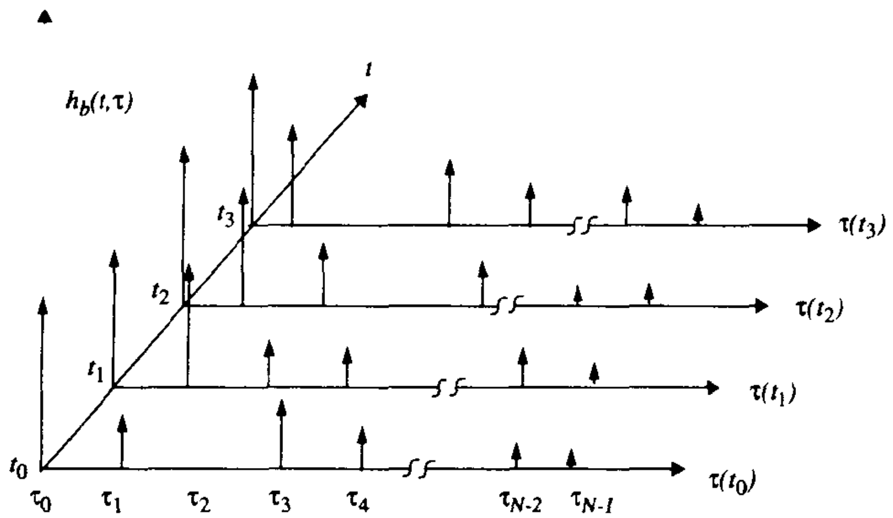

Figure 4.4
An example of the time varying discrete-time impulse response model for a multipath radio channel.

If the channel impulse response is assumed to be time invariant, or is at least wide sense stationary over a small-scale time or distance interval, then the channel impulse response may be simplified as

$$h_b(\tau) = \sum_{i=0}^{N-1} a_i \exp(-j\theta_i)\,\delta(\tau-\tau_i) \tag{4.13}$$

When measuring or predicting $h_b(\tau)$, a probing pulse $p(t)$ which approximates a delta function is used at the transmitter. That is

$$p(t) \approx \delta(t-\tau) \tag{4.14}$$

is used to sound the channel to determine $h_b(\tau)$.

For small-scale channel modeling, the *power delay profile* of the channel is found by taking the spatial average of $|h_b(t;\tau)|^2$ over a local area. By making several local area measurements of $|h_b(t;\tau)|^2$ in different locations, it is possible to build an ensemble of power delay profiles, each one representing a possible small-scale multipath channel state [Rap91a].

Based on work by Cox [Cox72], [Cox75], if $p(t)$ has a time duration much smaller than the impulse response of the multipath channel, $p(t)$ does not need to be deconvolved from the received signal $r(t)$ in order to determine relative multipath signal strengths. The received power delay profile in a local area is given by

$$P(t;\tau) \approx k|h_b(t;\tau)|^2 \tag{4.15}$$

and many snapshots of $|h_b(t;\tau)|^2$ are typically averaged over a local (small-scale) area to provide a single time-invariant multipath power delay profile $P(\tau)$. The gain k in equation (4.15) relates the transmitted power in the probing pulse $p(t)$ to the total power received in a multipath delay profile.

4.2.1 Relationship Between Bandwidth and Received Power

In actual wireless communication systems, the impulse response of a multipath channel is measured in the field using channel sounding techniques. We now consider two extreme channel sounding cases as a means of demonstrating how the small-scale fading behaves quite differently for two signals with different bandwidths in the identical multipath channel.

Consider a pulsed, transmitted RF signal of the form

$$x(t) = \mathrm{Re}\{p(t)\exp(j2\pi f_c t)\}$$

where $p(t)$ is a repetitive baseband pulse train with very narrow pulse width T_{bb} and repetition period T_{REP} which is much greater than the maximum measured excess delay τ_{max} in the channel. Now let

$$p(t) = 2\sqrt{\tau_{max}/T_{bb}} \text{ for } 0 \le t \le T_{bb}$$

surements (e.g., indoor channel sounding). Another limitation with this system is the non-real-time nature of the measurement. For time varying channels, the channel frequency response can change rapidly, giving an erroneous impulse response measurement. To mitigate this effect, fast sweep times are necessary to keep the total swept frequency response measurement interval as short as possible. A faster sweep time can be accomplished by reducing the number of frequency steps, but this sacrifices time resolution and excess delay range in the time domain. The swept frequency system has been used successfully for indoor propagation studies by Pahlavan [Pah95] and Zaghloul, et.al. [Zag91a], [Zag91b].

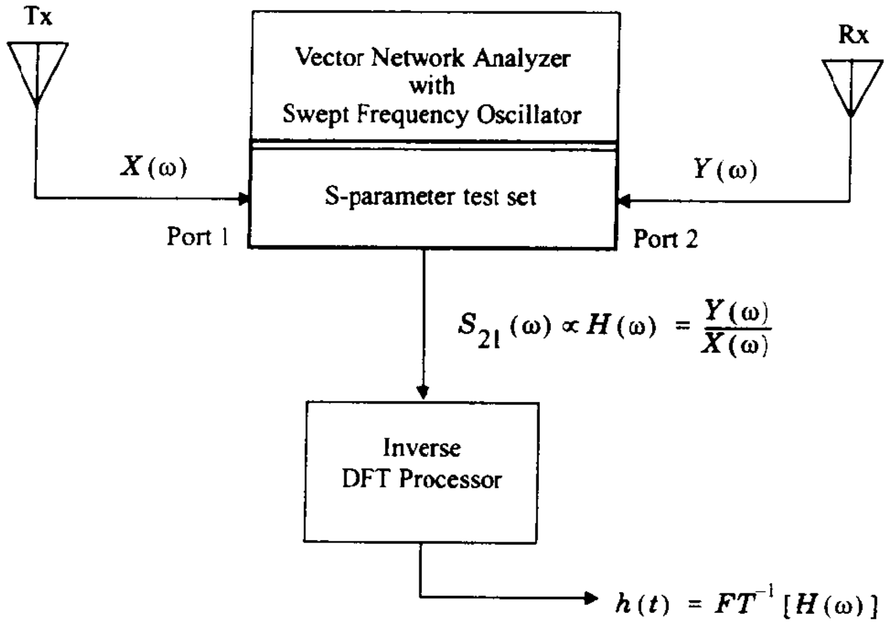

Figure 4.8
Frequency domain channel impulse response measurement system.

4.4 Parameters of Mobile Multipath Channels

Many multipath channel parameters are derived from the power delay profile, given by equation (4.18). Power delay profiles are measured using the techniques discussed in Section 4.4 and are generally represented as plots of relative received power as a function of excess delay with respect to a fixed time delay reference. Power delay profiles are found by averaging instantaneous power delay profile measurements over a local area in order to determine an average small-scale power delay profile. Depending on the time resolution of the probing pulse and the type of multipath channels studied, researchers often choose to sample at spatial separations of a quarter of a wavelength and over receiver movements no greater than 6 m in outdoor channels and no greater than 2 m in indoor channels in the 450 MHz - 6 GHz range. This small-scale sampling avoids large-scale averaging bias in the resulting small-scale statistics. Figure 4.9 shows typical power delay profile plots from outdoor and indoor channels, determined from a large number of closely sampled instantaneous profiles.

4.4.1 Time Dispersion Parameters

In order to compare different multipath channels and to develop some general design guidelines for wireless systems, parameters which grossly quantify the multipath channel are used. The *mean excess delay, rms delay spread,* and *excess delay spread (X* dB*)* are multipath channel parameters that can be determined from a power delay profile. The time dispersive properties of wide band multipath channels are most commonly quantified by their mean excess delay ($\bar{\tau}$) and rms delay spread (σ_τ). The mean excess delay is the first moment of the power delay profile and is defined to be

$$\bar{\tau} = \frac{\sum_k a_k^2 \tau_k}{\sum_k a_k^2} = \frac{\sum_k P(\tau_k)\tau_k}{\sum_k P(\tau_k)} \tag{4.35}$$

The rms delay spread is the square root of the second central moment of the power delay profile and is defined to be

$$\sigma_\tau = \sqrt{\overline{\tau^2} - (\bar{\tau})^2} \tag{4.36}$$

where

$$\overline{\tau^2} = \frac{\sum_k a_k^2 \tau_k^2}{\sum_k a_k^2} = \frac{\sum_k P(\tau_k)\tau_k^2}{\sum_k P(\tau_k)} \tag{4.37}$$

These delays are measured relative to the first detectable signal arriving at the receiver at $\tau_0 = 0$. Equations (4.35) - (4.37) do not rely on the absolute power level of $P(\tau)$, but only the relative amplitudes of the multipath components within $P(\tau)$. Typical values of rms delay spread are on the order of microseconds in outdoor mobile radio channels and on the order of nanoseconds in indoor radio channels. Table 4.1 shows the typical measured values of rms delay spread.

It is important to note that the rms delay spread and mean excess delay are defined from a single power delay profile which is the temporal or spatial average of consecutive impulse response measurements collected and averaged over a local area. Typically, many measurements are made at many local areas in order to determine a statistical range of multipath channel parameters for a mobile communication system over a large-scale area [Rap90].

The *maximum excess delay (X* dB*)* of the power delay profile is defined to be the time delay during which multipath energy falls to X dB below the maxi-

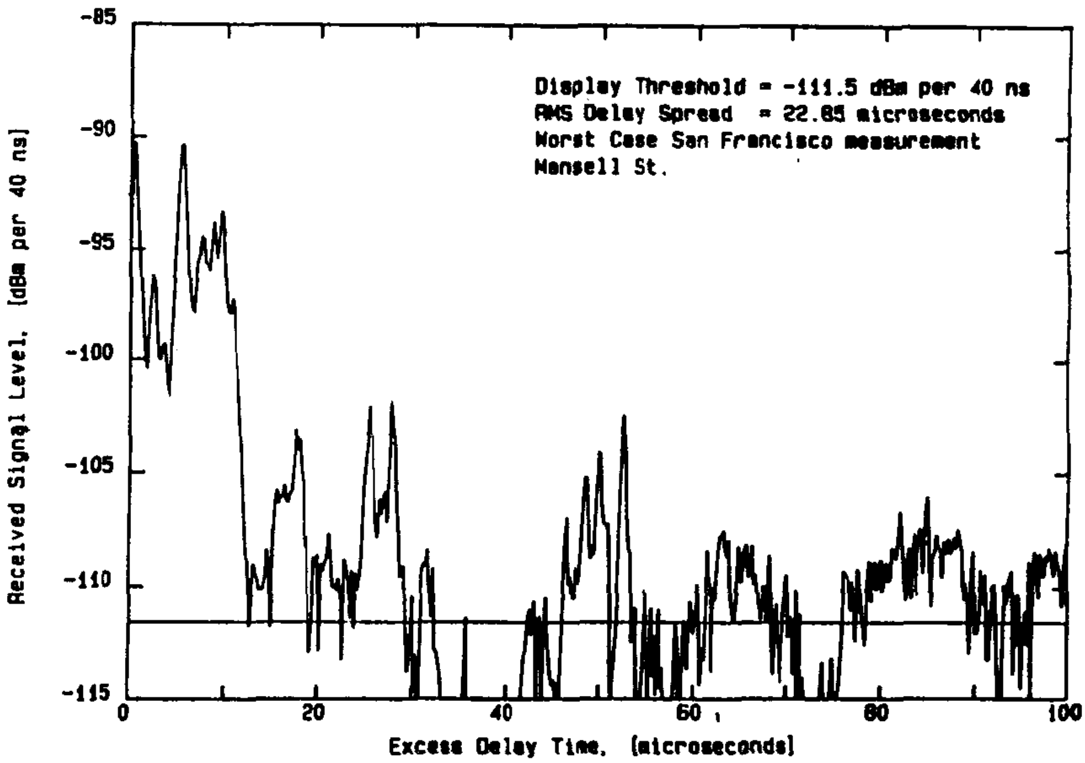

(a)

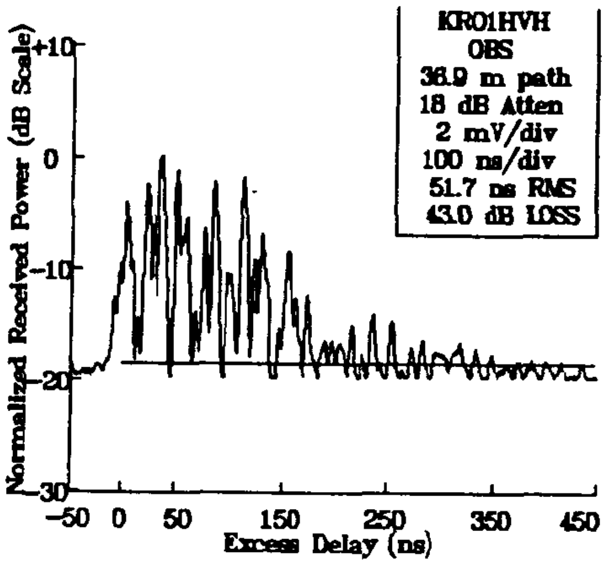

(b)

Figure 4.9
Measured multipath power delay profiles
a) From a 900 MHz cellular system in San Francisco [From [Rap90] © IEEE].
b) Inside a grocerv store at 4 GHz [From [Haw91] © IEEE].

Table 4.1 Typical Measured Values of RMS Delay Spread

Environment	Frequency (MHz)	RMS Delay Spread (σ_τ)	Notes	Reference
Urban	910	1300 ns avg. 600 ns st. dev. 3500 ns max.	New York City	[Cox75]
Urban	892	10-25 μs	Worst case San Francisco	[Rap90]
Suburban	910	200-310 ns	Averaged typical case	[Cox72]
Suburban	910	1960-2110 ns	Averaged extreme case	[Cox72]
Indoor	1500	10-50 ns 25 ns median	Office building	[Sal87]
Indoor	850	270 ns max.	Office building	[Dev90a]
Indoor	1900	70-94 ns avg. 1470 ns max.	Three San Francisco buildings	[Sei92a]

mum. In other words, the maximum excess delay is defined as $\tau_X - \tau_0$, where τ_0 is the first arriving signal and τ_X is the maximum delay at which a multipath component is within X dB of the strongest arriving multipath signal (which does not necessarily arrive at τ_0). Figure 4.10 illustrates the computation of the maximum excess delay for multipath components within 10 dB of the maximum. The maximum excess delay (X dB) defines the temporal extent of the multipath that is above a particular threshold. The value of τ_X is sometimes called the *excess delay spread* of a power delay profile, but in all cases must be specified with a threshold that relates the multipath noise floor to the maximum received multipath component.

In practice, values for $\bar{\tau}$, $\overline{\tau^2}$, and σ_τ depend on the choice of noise threshold used to process $P(\tau)$. The noise threshold is used to differentiate between received multipath components and thermal noise. If the noise threshold is set too low, then noise will be processed as multipath, thus giving rise to values of $\bar{\tau}$, $\overline{\tau^2}$, and σ_τ that are artificially high.

It should be noted that the power delay profile and the magnitude frequency response (the spectral response) of a mobile radio channel are related through the Fourier transform. It is therefore possible to obtain an equivalent description of the channel in the frequency domain using its frequency response characteristics. Analogous to the delay spread parameters in the time domain, *coherence bandwidth* is used to characterize the channel in the frequency domain. The rms delay spread and coherence bandwidth are inversely proportional to one another, although their exact relationship is a function of the exact multipath structure.

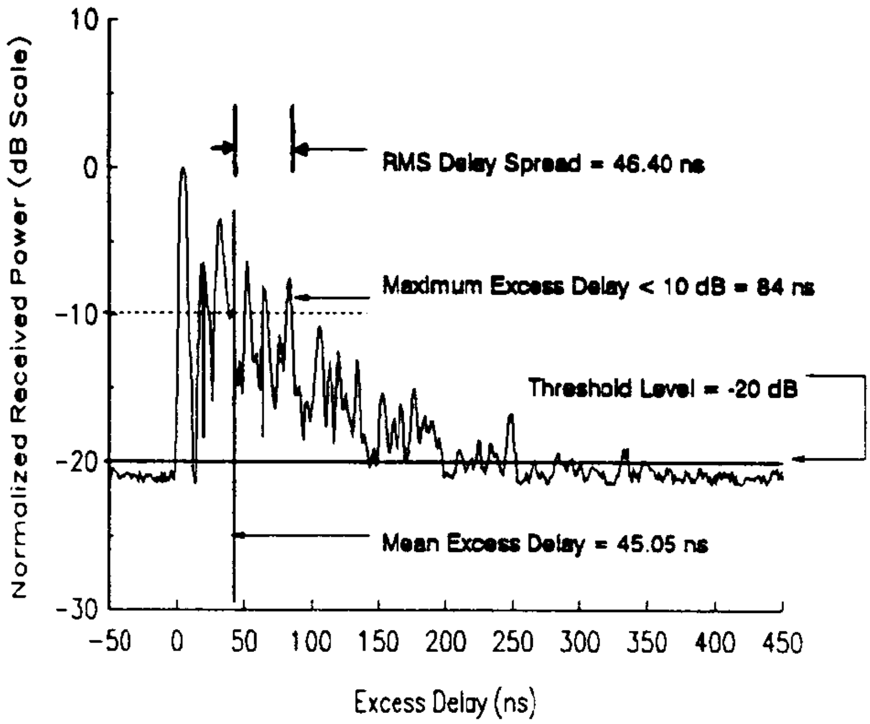

Figure 4.10
Example of an indoor power delay profile; rms delay spread, mean excess delay, maximum excess delay (10 dB), and threshold level are shown.

4.4.2 Coherence Bandwidth

While the delay spread is a natural phenomenon caused by reflected and scattered propagation paths in the radio channel, the coherence bandwidth, B_c, is a defined relation derived from the rms delay spread. Coherence bandwidth is a statistical measure of the range of frequencies over which the channel can be considered "flat" (i.e., a channel which passes all spectral components with approximately equal gain and linear phase). In other words, coherence bandwidth is the range of frequencies over which two frequency components have a strong potential for amplitude correlation. Two sinusoids with frequency separation greater than B_c are affected quite differently by the channel. If the coherence bandwidth is defined as the bandwidth over which the frequency correlation function is above 0.9, then the coherence bandwidth is approximately [Lee89b]

$$B_c \approx \frac{1}{50\sigma_\tau} \tag{4.38}$$

If the definition is relaxed so that the frequency correlation function is above 0.5, then the coherence bandwidth is approximately

$$B_c \approx \frac{1}{5\sigma_\tau} \tag{4.39}$$

It is important to note that an exact relationship between coherence bandwidth and rms delay spread does not exist, and equations (4.38) and (4.39) are "ball park estimates". In general, spectral analysis techniques and simulation are required to determine the exact impact that time varying multipath has on a particular transmitted signal [Chu87], [Fun93], [Ste94]. For this reason, accurate multipath channel models must be used in the design of specific modems for wireless applications [Rap91a], [Woe94].

Example 4.4

Calculate the mean excess delay, rms delay spread, and the maximum excess delay (10 dB) for the multipath profile given in the figure below. Estimate the 50% coherence bandwidth of the channel. Would this channel be suitable for AMPS or GSM service without the use of an equalizer?

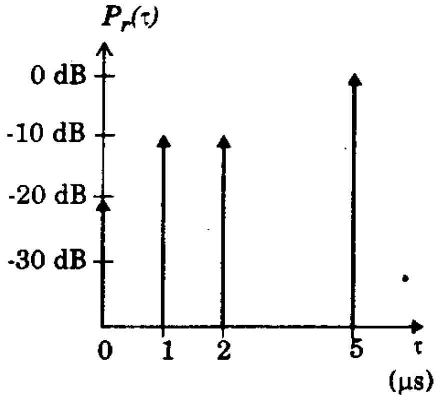

Figure E4.4

Solution to Example 4.4

The rms delay spread for the given multipath profile can be obtained using equations (4.35) — (4.37). The delays of each profile are measured relative to the first detectable signal. The mean excess delay for the given profile

$$\bar{\tau} = \frac{(1)(5) + (0.1)(1) + (0.1)(2) + (0.01)(0)}{[0.01 + 0.1 + 0.1 + 1]} = 4.38\mu s$$

The second moment for the given power delay profile can be calculated as

$$\overline{\tau^2} = \frac{(1)(5)^2 + (0.1)(1)^2 + (0.1)(2)^2 + (0.01)(0)}{1.21} = 21.07\mu s^2$$

Therefore the rms delay spread, $\sigma_\tau = \sqrt{21.07 - (4.38)^2} = 1.37\mu s$

The coherence bandwidth is found from equation (4.39) to be

$$B_c \approx \frac{1}{5\sigma_\tau} = \frac{1}{5(1.37\mu s)} = 146 \text{ kHz}$$

Since B_c is greater than 30 kHz, AMPS will work without an equalizer. However, GSM requires 200 kHz bandwidth which exceeds B_c, thus an equalizer would be needed for this channel.

4.4.3 Doppler Spread and Coherence Time

Delay spread and coherence bandwidth are parameters which describe the time dispersive nature of the channel in a local area. However, they do not offer information about the time varying nature of the channel caused by either relative motion between the mobile and base station, or by movement of objects in the channel. *Doppler spread* and *coherence time* are parameters which describe the time varying nature of the channel in a small-scale region.

Doppler spread B_D is a measure of the spectral broadening caused by the time rate of change of the mobile radio channel and is defined as the range of frequencies over which the received Doppler spectrum is essentially non-zero. When a pure sinusoidal tone of frequency f_c is transmitted, the received signal spectrum, called the Doppler spectrum, will have components in the range $f_c - f_d$ to $f_c + f_d$, where f_d is the Doppler shift. The amount of spectral broadening depends on f_d which is a function of the relative velocity of the mobile, and the angle θ between the direction of motion of the mobile and direction of arrival of the scattered waves. *If the baseband signal bandwidth is much greater than B_D, the effects of Doppler spread are negligible at the receiver.* This is a *slow* fading channel.

Coherence time T_c is the time domain dual of Doppler spread and is used to characterize the time varying nature of the frequency dispersiveness of the channel in the time domain. The Doppler spread and coherence time are inversely proportional to one another. That is,

$$T_C \approx \frac{1}{f_m} \tag{4.40.a}$$

Coherence time is actually a statistical measure of the time duration over which the channel impulse response is essentially invariant, and quantifies the similarity of the channel response at different times. In other words, coherence time is the time duration over which two received signals have a strong potential for amplitude correlation. If the reciprocal bandwidth of the baseband signal is greater than the coherence time of the channel, then the channel will change during the transmission of the baseband message, thus causing distortion at the receiver. If the coherence time is defined as the time over which the time correlation function is above 0.5, then the coherence time is approximately [Ste94]

$$T_C \approx \frac{9}{16\pi f_m} \tag{4.40.b}$$

where f_m is the maximum Doppler shift given by $f_m = v/\lambda$. In practice, (4.40.a) suggests a time duration during which a Rayleigh fading signal may fluctuate wildly, and (4.40.b) is often too restrictive. A popular rule of thumb for modern digital communications is to define the coherence time as the geometric mean of equations (4.40.a) and (4.40.b). That is,

$$T_C = \sqrt{\frac{9}{16\pi f_m^2}} = \frac{0.423}{f_m} \tag{4.40.c}$$

The definition of coherence time implies that two signals arriving with a time separation greater than T_C are affected differently by the channel. For example, for a vehicle traveling 60 mph using a 900 MHz carrier, a conservative value of T_C can be shown to be 2.22 ms from (4.40.b). If a digital transmission system is used, then as long as the symbol rate is greater than $1/T_C = 454$ bps, the channel will not cause distortion due to motion (however, distortion could result from multipath time delay spread, depending on the channel impulse response). Using the practical formula of (4.40.c), $T_C = 6.77$ ms and the symbol rate must exceed 150 bits/s in order to avoid distortion due to frequency dispersion.

Example 4.5

Determine the proper spatial sampling interval required to make small-scale propagation measurements which assume that consecutive samples are highly correlated in time. How many samples will be required over 10 m travel distance if $f_c = 1900$ MHz and $v = 50$ m/s. How long would it take to make these measurements, assuming they could be made in real time from a moving vehicle? What is the Doppler spread B_D for the channel?

Solution to Example 4.5

For correlation, ensure that the time between samples is equal to $T_C/2$, and use the smallest value of T_C for conservative design.
Using equation (4.40.b)

$$T_C \approx \frac{9}{16\pi f_m} = \frac{9\lambda}{16\pi v} = \frac{9c}{16\pi v f_c} = \frac{9 \times 3 \times 10^8}{16 \times 3.14 \times 50 \times 1900 \times 10^6}$$

$$T_C = 565\mu s$$

Taking time samples at less than half T_C, at $282.5\mu s$ corresponds to a spatial sampling interval of

$$\Delta x = \frac{vT_C}{2} = \frac{50 \times 565\mu s}{2} = 0.014125 \text{ m} = 1.41 \text{ cm}$$

Therefore, the number of samples required over a 10 m travel distance is

$$N_x = \frac{10}{\Delta x} = \frac{10}{0.014125} = 708 \text{ samples}$$

The time taken to make this measurement is equal to $\frac{10\text{m}}{50 \text{ m/s}} = 0.2$ s
The Doppler spread is

$$B_D = f_m = \frac{vf_c}{c} = \frac{50 \times 1900 \times 10^6}{3 \times 10^8} = 316.66 \text{ Hz}$$

4.5 Types of Small-Scale Fading

Section 4.3 demonstrated that the type of fading experienced by a signal propagating through a mobile radio channel depends on the nature of the transmitted signal with respect to the characteristics of the channel. Depending on the relation between the signal parameters (such as bandwidth, symbol period, etc.) and the channel parameters (such as rms delay spread and Doppler spread), different transmitted signals will undergo different types of fading. The time dispersion and frequency dispersion mechanisms in a mobile radio channel lead to four possible distinct effects, which are manifested depending on the nature of the transmitted signal, the channel, and the velocity. While multipath delay spread leads to *time dispersion* and *frequency selective fading*, Doppler spread leads to *frequency dispersion* and *time selective fading*. The two propagation mechanisms are independent of one another. Figure 4.11 shows a tree of the four different types of fading.

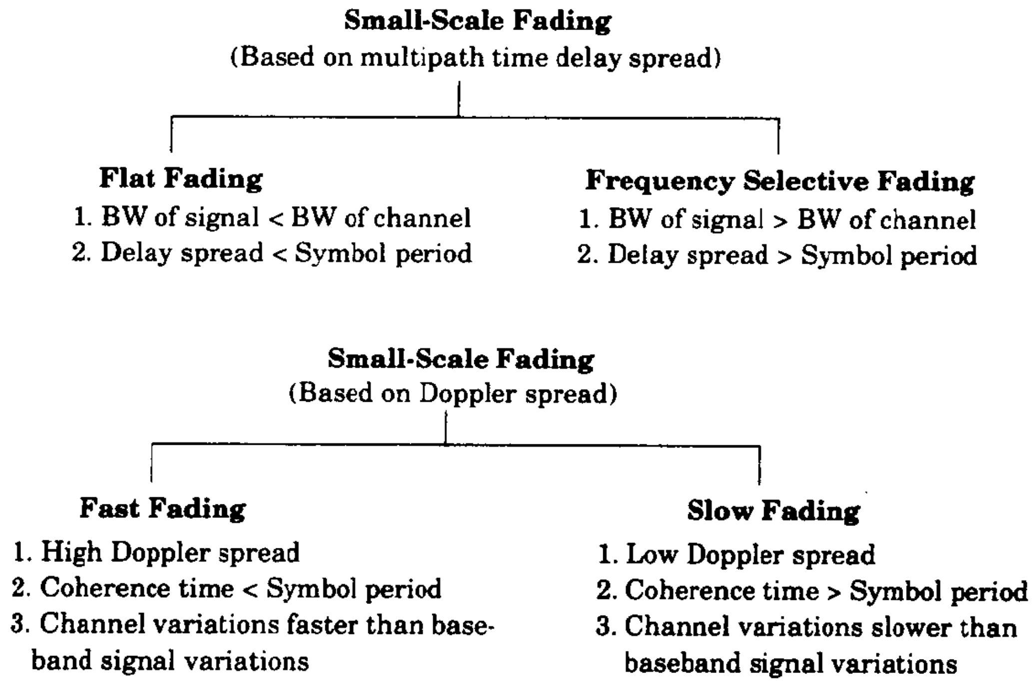

Figure 4.11
Types of small-scale fading.

4.5.1 Fading Effects Due to Multipath Time Delay Spread

Time dispersion due to multipath causes the transmitted signal to undergo either flat or frequency selective fading.

4.5.1.1 Flat fading

If the mobile radio channel has a constant gain and linear phase response over a bandwidth which is greater than the bandwidth of the transmitted signal, then the received signal will undergo *flat fading*. This type of fading is historically the most common type of fading described in the technical literature. In flat fading, the multipath structure of the channel is such that the spectral characteristics of the transmitted signal are preserved at the receiver. However the strength of the received signal changes with time, due to fluctuations in the gain of the channel caused by multipath. The characteristics of a flat fading channel are illustrated in Figure 4.12.

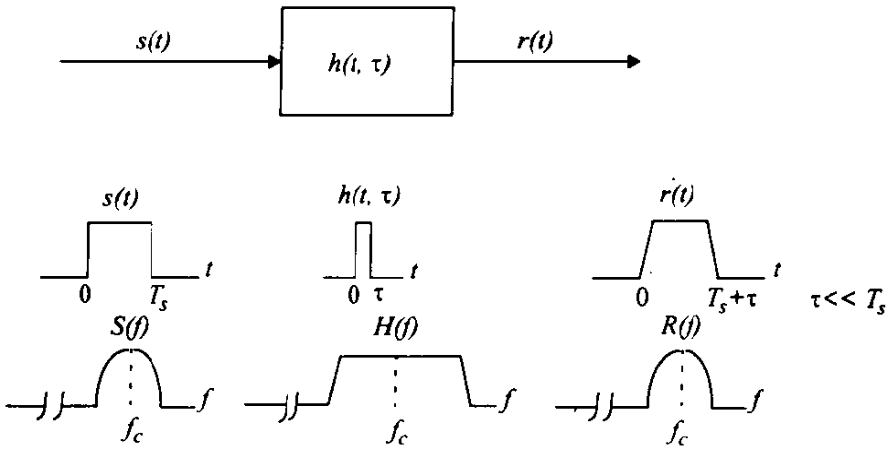

Figure 4.12
Flat fading channel characteristics.

It can be seen from Figure 4.12 that if the channel gain changes over time, a change of amplitude occurs in the received signal. Over time, the received signal $r(t)$ varies in gain, but the spectrum of the transmission is preserved. In a flat fading channel, the reciprocal bandwidth of the transmitted signal is much larger than the multipath time delay spread of the channel, and $h_b(t, \tau)$ can be approximated as having no excess delay (i.e., a single delta function with $\tau = 0$). Flat fading channels are also known as *amplitude varying channels* and are sometimes referred to as *narrowband channels*, since the bandwidth of the applied signal is *narrow* as compared to the channel flat fading bandwidth. Typical flat fading channels cause deep fades, and thus may require 20 or 30 dB more transmitter power to achieve low bit error rates during times of deep fades as compared to systems operating over non-fading channels. The distribution of the instantaneous gain of flat fading channels is important for designing radio links, and the most common amplitude distribution is the Rayleigh distribution. The Rayleigh flat fading channel model assumes that the channel induces an amplitude which varies in time according to the Rayleigh distribution.

To summarize, a signal undergoes flat fading if

$$B_S \ll B_C \tag{4.41}$$

and

$$T_S \gg \sigma_\tau \tag{4.42}$$

where T_S is the reciprocal bandwidth (e.g., symbol period) and B_S is the bandwidth, respectively, of the transmitted modulation, and σ_τ and B_C are the rms delay spread and coherence bandwidth, respectively, of the channel.

4.5.1.2 Frequency Selective Fading

If the channel possesses a constant-gain and linear phase response over a bandwidth that is smaller than the bandwidth of transmitted signal, then the channel creates *frequency selective fading* on the received signal. Under such conditions the channel impulse response has a multipath delay spread which is greater than the reciprocal bandwidth of the transmitted message waveform. When this occurs, the received signal includes multiple versions of the transmitted waveform which are attenuated (faded) and delayed in time, and hence the received signal is distorted. Frequency selective fading is due to time dispersion of the transmitted symbols within the channel. Thus the channel induces *intersymbol interference* (ISI). Viewed in the frequency domain, certain frequency components in the received signal spectrum have greater gains than others.

Frequency selective fading channels are much more difficult to model than flat fading channels since each multipath signal must be modeled and the channel must be considered to be a linear filter. It is for this reason that wideband multipath measurements are made, and models are developed from these measurements. When analyzing mobile communication systems, statistical impulse response models such as the 2-ray Rayleigh fading model (which considers the impulse response to be made up of two delta functions which independently fade and have sufficient time delay between them to induce frequency selective fading upon the applied signal), or computer generated or measured impulse responses, are generally used for analyzing frequency selective small-scale fading. Figure 4.13 illustrates the characteristics of a frequency selective fading channel.

For frequency selective fading, the spectrum $S(f)$ of the transmitted signal has a bandwidth which is greater than the coherence bandwidth B_C of the channel. Viewed in the frequency domain, the channel becomes frequency selective, where the gain is different for different frequency components. Frequency selec-

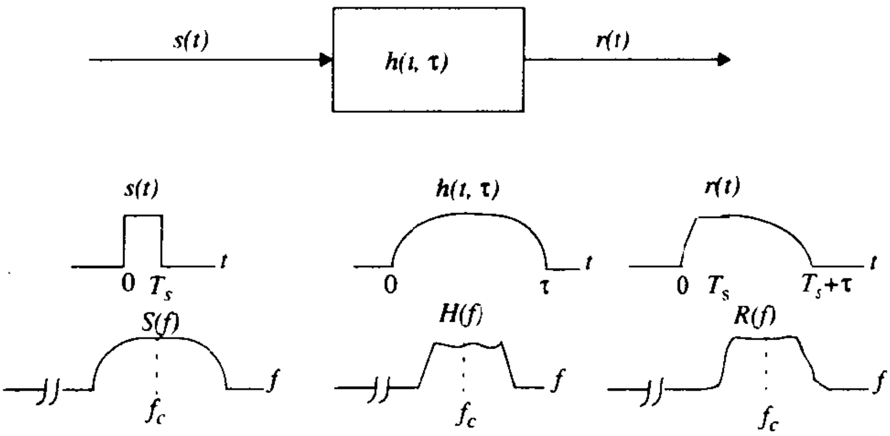

Figure 4.13
Frequency selective fading channel characteristics.

tive fading is caused by multipath delays which approach or exceed the symbol period of the transmitted symbol. Frequency selective fading channels are also known as *wideband channels* since the bandwidth of the signal $s(t)$ is wider than the bandwidth of the channel impulse response. As time varies, the channel varies in gain and phase across the spectrum of $s(t)$, resulting in time varying distortion in the received signal $r(t)$. To summarize, a signal undergoes frequency selective fading if

$$B_S > B_C \tag{4.43}$$

and

$$T_S < \sigma_\tau \tag{4.44}$$

A common rule of thumb is that a channel is frequency selective if $T_s \leq 10\sigma_\tau$, although this is dependent on the specific type of modulation used. Chapter 5 presents simulation results which illustrate the impact of time delay spread on bit error rate (BER).

4.5.2 Fading Effects Due to Doppler Spread

4.5.2.1 Fast Fading

Depending on how rapidly the transmitted baseband signal changes as compared to the rate of change of the channel, a channel may be classified either as a *fast fading* or *slow fading* channel. In a *fast fading channel*, the channel impulse response changes rapidly within the symbol duration. That is, the coherence time of the channel is smaller than the symbol period of the transmitted signal. This causes frequency dispersion (also called time selective fading) due to Doppler spreading, which leads to signal distortion. Viewed in the frequency domain, signal distortion due to fast fading increases with increasing Doppler spread relative to the bandwidth of the transmitted signal. Therefore, a signal undergoes fast fading if

$$T_S > T_C \tag{4.45}$$

and

$$B_S < B_D \tag{4.46}$$

It should be noted that when a channel is specified as a fast or slow fading channel, it does not specify whether the channel is flat fading or frequency selective in nature. Fast fading only deals with the rate of change of the channel due to motion. In the case of the flat fading channel, we can approximate the impulse response to be simply a delta function (no time delay). Hence, a *flat fading, fast fading* channel is a channel in which the amplitude of the delta function varies faster than the rate of change of the transmitted baseband signal. In the case of a *frequency selective, fast fading* channel, the amplitudes, phases, and time delays of any one of the multipath components vary faster than the rate of change of the transmitted signal. In practice, fast fading only occurs for very low data rates.

4.5.2.2 Slow Fading

In a *slow fading channel*, the channel impulse response changes at a rate much slower than the transmitted baseband signal *s(t)*. In this case, the channel may be assumed to be static over one or several reciprocal bandwidth intervals. In the frequency domain, this implies that the Doppler spread of the channel is much less than the bandwidth of the baseband signal. Therefore, a signal undergoes slow fading if

$$T_S \ll T_C \tag{4.47}$$

and

$$B_S \gg B_D \tag{4.48}$$

It should be clear that the velocity of the mobile (or velocity of objects in the channel) and the baseband signaling determines whether a signal undergoes fast fading or slow fading.

The relation between the various multipath parameters and the type of fading experienced by the signal are summarized in Figure 4.14. Over the years, some authors have confused the terms fast and slow fading with the terms large-scale and small-scale fading. It should be emphasized that fast and slow fading deal with the relationship between the time rate of change in the channel and the transmitted signal, and not with propagation path loss models.

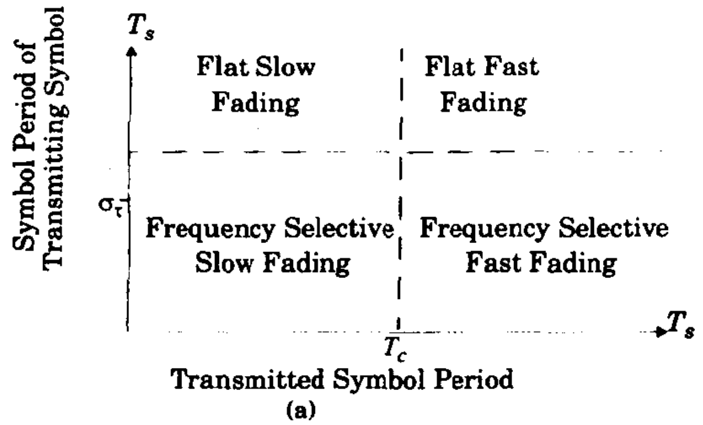

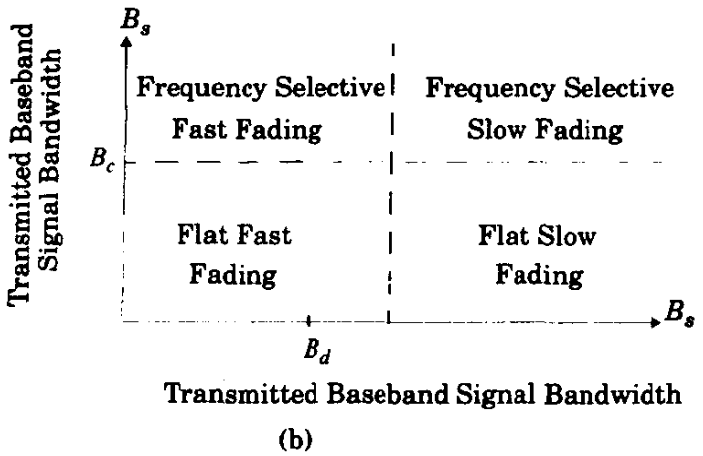

Figure 4.14
Matrix illustrating type of fading experienced by a signal as a function of
(a) symbol period
(b) baseband signal bandwidth.

4.6 Rayleigh and Ricean Distributions

4.6.1 Rayleigh Fading Distribution

In mobile radio channels, the Rayleigh distribution is commonly used to describe the statistical time varying nature of the received envelope of a flat fading signal, or the envelope of an individual multipath component. It is well known that the envelope of the sum of two quadrature Gaussian noise signals obeys a Rayleigh distribution. Figure 4.15 shows a Rayleigh distributed signal envelope as a function of time. The Rayleigh distribution has a probability density function (pdf) given by

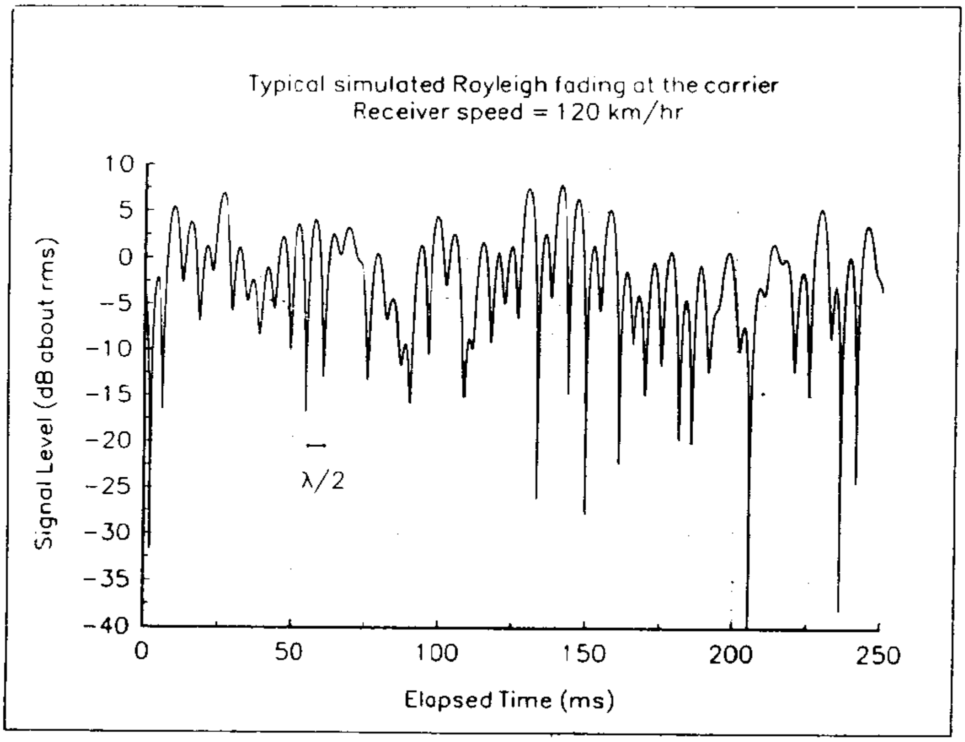

Figure 4.15
A typical Rayleigh fading envelope at 900 MHz [From [Fun93] © IEEE].

$$p(r) = \begin{cases} \frac{r}{\sigma^2}\exp\left(-\frac{r^2}{2\sigma^2}\right) & (0 \le r \le \infty) \\ 0 & (r < 0) \end{cases} \qquad (4.49)$$

where σ is the rms value of the received voltage signal before *envelope detection*, and σ^2 is the time-average power of the received signal *before* envelope detection. The probability that the envelope of the received signal does not exceed a specified value R is given by the corresponding cumulative distribution function (CDF)

$$P(R) = Pr(r \le R) = \int_0^R p(r)\,dr = 1 - \exp\left(-\frac{R^2}{2\sigma^2}\right) \qquad (4.50)$$

The mean value r_{mean} of the Rayleigh distribution is given by

$$r_{mean} = E[r] = \int_0^\infty rp(r)\,dr = \sigma\sqrt{\frac{\pi}{2}} = 1.2533\sigma \qquad (4.51)$$

and the variance of the Rayleigh distribution is given by σ_r^2, which represents the ac power in the signal envelope

$$\sigma_r^2 = E[r^2] - E^2[r] = \int_0^{\infty} r^2 p(r)\, dr - \frac{\sigma^2 \pi}{2} \tag{4.52}$$

$$= \sigma^2\left(2 - \frac{\pi}{2}\right) = 0.4292\sigma^2$$

The rms value of the envelope is the square root of the mean square, or $\sqrt{2}\sigma$.

The median value of r is found by solving

$$\frac{1}{2} = \int_0^{r_{median}} p(r)\, dr \tag{4.53}$$

and is

$$r_{median} = 1.177\sigma \tag{4.54}$$

Thus the mean and the median differ by only 0.55 dB in a Rayleigh fading signal. Note that the median is often used in practice, since fading data are usually measured in the field and a particular distribution cannot be assumed. By using median values instead of mean values it is easy to compare different fading distributions which may have widely varying means. Figure 4.16 illustrates the Rayleigh pdf. The corresponding Rayleigh cumulative distribution function (CDF) is shown in Figure 4.17.

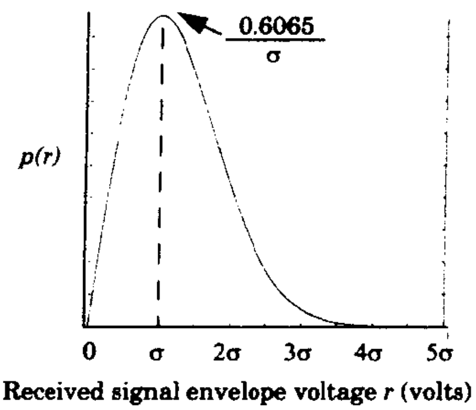

Figure 4.16
Rayleigh probability density function (pdf).

4.6.2 Ricean Fading Distribution

When there is a dominant stationary (nonfading) signal component present, such as a line-of-sight propagation path, the small-scale fading envelope

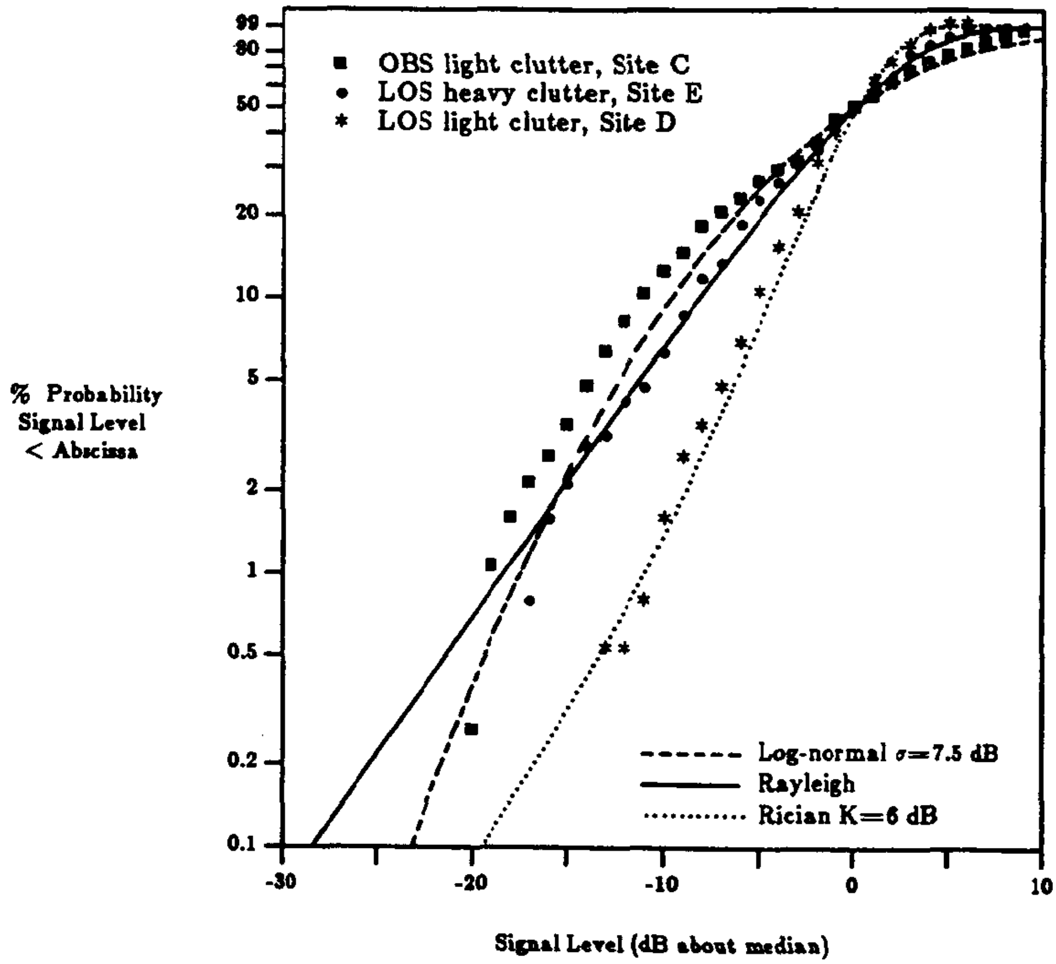

Figure 4.17
Cumulative distribution for three small-scale fading measurements and their fit to Rayleigh, Ricean, and log-normal distributions [From [Rap89] © IEEE].

distribution is Ricean. In such a situation, random multipath components arriving at different angles are superimposed on a stationary dominant signal. At the output of an envelope detector, this has the effect of adding a dc component to the random multipath.

Just as for the case of detection of a sine wave in thermal noise [Ric48], the effect of a dominant signal arriving with many weaker multipath signals gives rise to the Ricean distribution. As the dominant signal becomes weaker, the composite signal resembles a noise signal which has an envelope that is Rayleigh. Thus, the Ricean distribution degenerates to a Rayleigh distribution when the dominant component fades away.

The Ricean distribution is given by

$$p(r) = \begin{cases} \frac{r}{\sigma^2} e^{-\frac{(r^2 + A^2)}{2\sigma^2}} I_0\left(\frac{Ar}{\sigma^2}\right) & \text{for } (A \geq 0, r \geq 0) \\ 0 & \text{for } (r < 0) \end{cases} \tag{4.55}$$

The parameter A denotes the peak amplitude of the dominant signal and $I_0(\cdot)$ is the modified Bessel function of the first kind and zero-order. The Ricean distribution is often described in terms of a parameter K which is defined as the ratio between the deterministic signal power and the variance of the multipath. It is given by $K = A^2/(2\sigma^2)$ or, in terms of dB

$$K(\text{dB}) = 10\log\frac{A^2}{2\sigma^2} \text{ dB} \tag{4.56}$$

The parameter K is known as the Ricean factor and completely specifies the Ricean distribution. As $A \to 0, K \to -\infty$ dB, and as the dominant path decreases in amplitude, the Ricean distribution degenerates to a Rayleigh distribution. Figure 4.18 shows the Ricean pdf. The Ricean CDF is compared with the Rayleigh CDF in Figure 4.17.

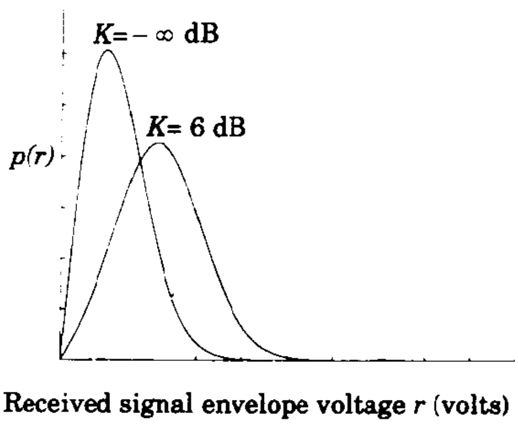

Figure 4.18
Probability density function of Ricean distributions: $K = -\infty$ dB (Rayleigh) and $K = 6$ dB. For $K \gg 1$, the Ricean pdf is approximately Gaussian about the mean.

4.7 Statistical Models for Multipath Fading Channels

Several multipath models have been suggested to explain the observed statistical nature of a mobile channel. The first model presented by Ossana [Oss64] was based on interference of waves incident and reflected from the flat sides of randomly located buildings. Although Ossana's model [Oss64] predicts flat fading power spectra that were in agreement with measurements in suburban